Teknik Dergi, 2021 10629-10643, Paper 606

Acceleration Displacement Response Spectra for Design of Seismic Isolation Systems in Turkey

Aslıhan YOLCU[1]
Gülüm TANIRCAN[2]
Cüneyt TÜZÜN[3]

ABSTRACT

In this study, base shear and inelastic displacement limits of seismic isolation systems are presented through acceleration-displacement response spectra considering the ground motion and design provisions of the Turkish Building Seismic Design Code. A series of nonlinear response history analyses are performed using a combination of eight site-specific design spectra, six isolation systems having six different periods and five yield levels. As a result, eight spectra presented herein can be used for the preliminary design stage of seismic isolation systems in Turkey.

Keywords: Seismic isolation, non-linear response history analysis, acceleration-displacement response spectrum.

1. INTRODUCTION

The impact of two devastating earthquakes in Turkey in 1999 has revealed not only the existence of many structures that are not in compliance with seismic regulations but also nationwide belated implementation of advanced technologies for earthquake resistant design. Until 1999, application of isolation systems was limited to a few viaducts in Turkey. Istanbul Airport terminal building is the first building that has been reinforced by using isolators (friction pendulum bearings) at the time of the 1999 earthquakes. Over the past 19 years the number of applications has increased both for reinforcement of existing structures and for design of new structures. According to the database of Turkish Association for Seismic Isolation, as of 2018, number of base isolated structures including airports, hospitals, industrial structures as well as residential buildings are over 125 [1]. As the use of seismic

Note:
- This paper has been received on January 11, 2019 and accepted for publication by the Editorial Board on December 4, 2019.
- Discussions on this paper will be accepted by May 31, 2021.
- https://dx.doi.org/10.18400/tekderg.511798

1 Bogazici University, Kandilli Observatory and Earthquake Research Institute, Istanbul, Turkey - aslihanyolcu@hotmail.com - https://orcid.org/0000-0002-4096-1215

2 Bogazici University, Kandilli Observatory and Earthquake Research Institute, Istanbul, Turkey - birgore@boun.edu.tr - https://orcid.org/0000-0002-0535-5658

3 Gebze Technical University, Department of Civil Engineering, Kocaeli, Turkey - ctuzun@gmail.com https://orcid.org/0000-0003-2489-2640

isolation has become more widespread, seismic design criteria of isolation systems/isolated buildings have been accorded a separate chapter of the most recent Turkish Building Seismic Design Code (hereafter; TBSDR-2018) [2].

According to the provision in the most current seismic design codes (*e.g*. [2, 3]) isolation systems should be designed considering their nonlinear characteristics under maximum considered earthquake ground motion. Hysteretic behaviour of the seismic isolation systems can be defined in accordance with an equivalent linear system with secant stiffness and an equivalent viscous damping approach (*e.g.* [4, 5]). Effective stiffness, effective period and effective damping ratio are the major properties of an equivalent linear system. The major obstacle in implementing force-displacement hysteresis during the preliminary design of the seismic isolation system is that those properties are response displacement amplitude dependent and hence determining the acceptable displacement response values for the design requires an iterative procedure. In this context, as an alternative to equivalent linear analysis method, time history analysis method has also been practiced by many researchers for the design of isolation systems.

Looking through research in this direction, Park and Otsuka [6] applied the nonlinear response spectrum approach to investigate the optimal yield level of isolation systems for bridges. Tena-Colunga [7] proposed inelastic capacity design spectra of isolation systems for fixed yield strength and post yield stiffness. Ryan and Chopra [8] offered an alternative procedure for the iterative equivalent linear methods by reducing the parameters of equation of motion as presented in the next section. Whittaker and Jones [9, 10] proposed the concept of acceleration-displacement response spectra (ADRS). The concept is based on time history analyses of inelastic single degree of freedom (SDOF) oscillator to represent the nonlinear behaviour of the isolation systems. Properties of seismic isolation systems are independent of amplitude and can be selected by designers in the preliminary design process. Hence, the concept helps designers to develop quickly an estimate of the inelastic seismic demands of seismically isolated systems [11]. The concept has been applied to Christchurch-New Zealand, Vancouver-Canada, San Francisco Bay area-USA and Chile based on relevant codes [11] [12]. This concept has also been performed for two specific structures in Istanbul and Erzurum–Turkey following ASCE 7-10 [13] provisions [14]. However, none of the above studies considers different seismic input levels and site classes.

The main objective of this paper is to calculate and present the ADRS graphs considering the ground motion and building seismic design provisions of Turkey [2]. The ADRS approach is applied to high and moderate seismic zones of Turkey using different combinations of two earthquake ground motion levels (maximum considered earthquake: DD1 and design basis earthquake: DD2) and two site categories (stiff sites: ZC, and soil sites: ZD). For each category eleven pairs of ground motion recordings are selected from PEER-West2 [15] worldwide earthquake catalogue and linearly scaled to fit the pre-defined design spectra. A wide range of period (2-5 seconds) and yield strength ratio (5% -15% of W) are used to represent a broad envelope which includes not only the practical and applicable period and strength ratio levels but also extreme values of them for an isolation system. Results are discussed in the following parts of the paper. Finally, conclusions are drawn based on the obtained results. Hence, this study can be evaluated as a general approach for preliminary design of seismic isolation systems proposed for Turkey for the first time.

2. METHODOLOGY

Seismic isolation system can be idealized as a SDOF oscillator with a rigid mass on a single isolator. A bi-linear characterization of force-displacement hysteresis curve which can be considered as the envelope of isolation system response, is used for more practice-oriented representation of the nonlinear behaviour of a typical seismic isolation system in a horizontal direction as given in Fig. 1. In the figure, zero displacement force intercept (Q_d) expresses characteristic strength of a seismic isolator. F_y is the yield force. First and second slopes of the force-displacement graph are the elastic stiffness (k_1) and characteristic stiffness (k_2) of the seismic isolation system, respectively. In general applications, k_2 is taken as a fraction of k_1 [16]. Effective stiffness (k_e) is the secant slope of the simplified maximum response and is a function of maximum displacement.

Among all parameters defining the hysteresis loop, k_2 and Q_d are dependent only on material properties (*e.g.* shear modulus of rubber and yield shear stress of lead for lead rubber bearings) and geometric features (*e.g.* radius of friction pendulum systems, cross section area and thickness of lead rubber bearings) of isolation systems. Ryan and Chopra [8] simplified calculation of the equation of motion by utilizing $\omega = \sqrt{k_2 / m_t}$ and yield (or characteristic) strength ratio (Q_d /W), where W is the weight acting on the system.

The deformation history of the isolator $u(t)$, subjected to ground acceleration $\ddot{u}_g(t)$, is governed by the Equation 1;

$$\ddot{u}(t) + \omega^2 u(t) + (Qd\ /W)\ g\ z(t, k, u, \dot{u}) = -\ddot{u}_g(t), \tag{1}$$

where g is acceleration due to gravity and z represents the yielding history. Also, $\ddot{u}(t)$ shows isolator acceleration when m_t represents the mass. Moreover t, k, u and $\dot{u}$ are time, stiffness, displacement and velocity, respectively.

Computation of the ADRS graphs consists of two major steps: Preparation of horizontal ground motion excitations in compliance with TBSDR-2018 [2] and calculation of deformation history of a nonlinear SDOF system for various ground motion pairs with predefined hysteretic model parameters. Nonlinear time history analyses are performed for various post yield stiffness period of the isolation system (T), Q_d /W and k_2 combinations to obtain the displacement response. Finally, base shear transmitted to superstructure can be found out;

$$V_M = \frac{S_{ae}^{DD1}(T_M) W \eta_M}{R} \tag{2}$$

In the Equation 2, S_{ae}^{DD1} is 5% damped spectral acceleration parameter at effective vibration period (T_M) of the isolation system under DD1 ground motion level. T_M corresponds to the period where the maximum displacement of the isolation system is obtained. Earthquake force reduction factors (R) are tabulated in design codes for desired performance levels. Damping scaling coefficient (η_M) can be calculated by the following equation [2, 17, 18];

$$\eta = \sqrt{\frac{10}{5+\xi}} \tag{3}$$

where ξ is effective damping ratio and it shows the damping ratio as a percent. Parameters for calculation of ξ, vary depending on the type of the isolation system. In this research calculations follow straightforward design concept of friction type isolator.

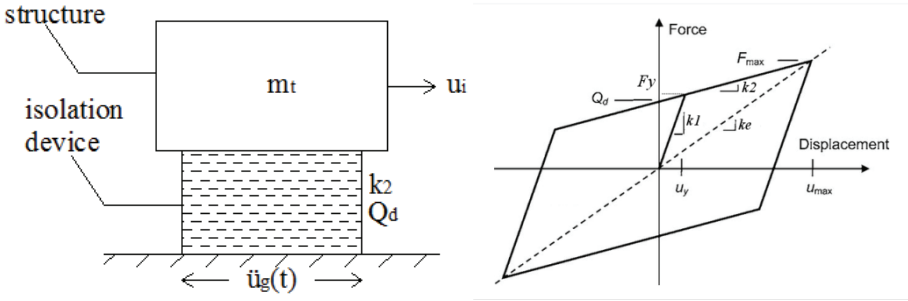

Figure 1 - (left) Seismic isolation system representation (adapted from Ryan and Chopra [8]); (right) Idealized bi-linear hysteretic response of isolators

3. GROUND MOTION REPRESENTATION

3.1. Selection of Hazard Levels

The capacity of an isolation system should be larger than strength and displacement demands of maximum considered earthquake ground motion (*e.g.* [2, 13]). Hence, in accordance with this performance expectation, nationwide distribution of the 5% damped spectral acceleration parameters at 1 s period (S_{a1}) is investigated. DD1 and DD2 (levels are provided from revised seismic hazard maps of Turkey [19, 20]. In order not to use the earthquake records which may contain near-field effects, the average values of S_{a1} are estimated in the regions at least 15 km from the fault. For the reference site condition, maximum S_{a1} value reaches 1.4 g at zero distance to major active faults and sharply decrease to 0.6 g at approximately 15-20 km away from the fault lines. It further decreases to 0.4 g at 45-50 km epicentral distance (see Fig. 2). For those regions, the hazard is diversified into two levels; moderate hazard level (MH) (0.4 g≤ S_{a1} (DD1) <0.5 g) and high hazard level (HH) (0.5 g≤ S_{a1} (DD1) <0.6 g). Aritmetic mean values of these ranges are used as representative values for calculating elastic response spectra. DD2 performance level is also required by the TBSDR-2018 [2] for calculating maximum shear forces transferred to structure above the isolator. Therefore, corresponding representative average S_{a1} values at DD2 level are chosen compatible with S_{a1} values at DD1 level as 0.30 g and 0.25 g for high and moderate hazard regions, respectively. Case numbers are assigned to eight hazard levels for easy follow-up of the results (Table 1).

Table 1 - Cases for ground motion levels formed by the combination of design, hazard and site categories

	Case1	Case2	Case3	Case4	Case5	Case6	Case7	Case8
Hazard Level	DD1	DD1	DD2	DD2	DD1	DD1	DD2	DD2
	MH	MH	MH	MH	HH	HH	HH	HH
Site Type	ZC	ZD	ZC	ZD	ZC	ZD	ZC	ZD

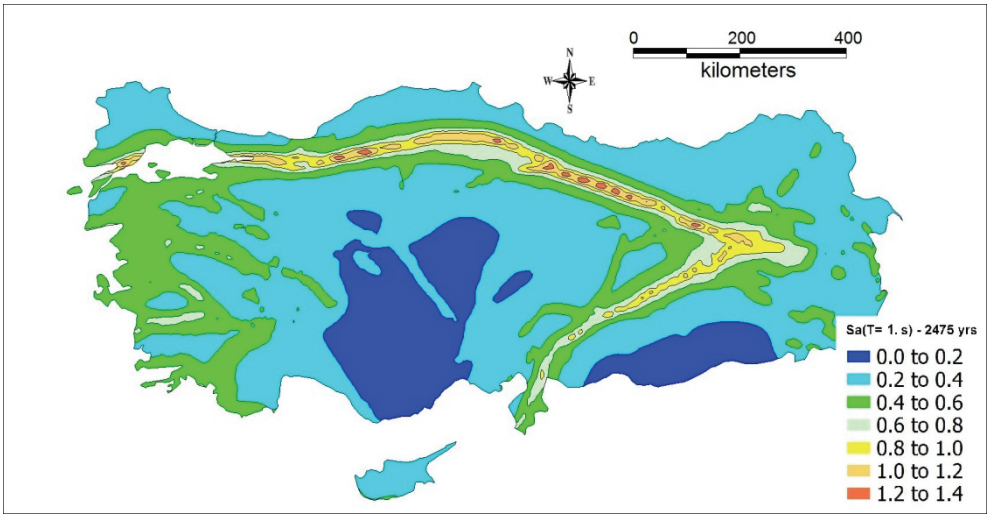

Figure 2 - Sa1 contour map at reference site conditions (Vs_{30}=760 m/s) for 2% probability of exceedance in 50 years exposure time (DD1 level) (redrawn after [19]).

3.2. Selection and Scaling of Strong Motion Recordings

30 strong motion recordings are selected from Pacific Earthquake Engineering Research (PEER) Center database [15]. The magnitude (Mw) range is assigned as 6.0 to 7.28 and style of faulting is strike slip considering the two major faulting zones exhibiting the highest seismic hazard in Turkey, the North Anatolian and the East Anatolian Fault Zone. The Distance (R_{jb}) between recording station and vertical projection of fault plane is chosen between 15 km - 60 km. List of earthquake ground motion pairs are tabulated in Table 2. 15 km distance is assumed to be the sufficient distance to neglect near field effects. Pulse-like recordings are ignored. Soil types belong to ZC (360 m/s $\leq V_{s30}<$ 760 m/s) and ZD (180 m/s $\leq V_{s30} <$ 360 m/s) categories. Eleven horizontal ground motion pairs are selected for each of eight groups which are formed by the combination of design, hazard and site categories. Maximum number of ground motion recordings from the same event for each of eight groups is three.

Following the provisions given in TBSDR-2018 [2] ground motion pairs are scaled linearly to match the 5% damped elastic horizontal design spectra. Geometric mean spectrum of selected ground motion pairs fit the horizontal elastic spectra between 1.4-7 s. period range. The same scaling factor is used for each horizontal component of a ground motion recording. The majority of scale factors takes values between 1-9. Two out of eleven scaling factors used for DD1/MH /ZC spectrum are as high as 14. Even though small scale values are recommended for linearly scaled ground motions, the effect of scaling factor and magnitude-distance bins on median nonlinear structural response for long period structures (T≤4 s) is found to be small and scale results are unbiased [21]. 5% damped elastic design spectra for DD1 and DD2 design levels are given together with elastic response spectra of selected and scaled recordings in Fig. 3.

3.3. Nonlinear SDOF Time History Analyses

Considering the bilinear hysteric model in Fig. 1, nonlinear time history analyses are performed for each scaled horizontal component of ground motions. PRISM software [22] is employed for the calculations. Assumptions and parameters for the calculation are as follows. Average k_2/k_1 is taken as 0.1 which is a common value for design purposes, provided by the manufacturers and obtained by prototype test results [17, 23]. Elastic damping ratio of bilinear oscillation is omitted, six periods of vibration (T = 2.0, 2.5, 3.0, 3.5, 4.0, 5.0 s) and five Q_d /W (5%, 7.5%, 10%, 12.5%, 15%) values are used. A total of 5280 nonlinear analyses are performed using 30 different bilinear hysteretic curves under the excitation of 11 different ground motion pairs produced for eight cases. Square root of the sum of the squares (SRSS) of two response displacements at period corresponding to the largest response displacement in horizontal direction, is calculated. The largest of the SRSS is considered as the maximum response displacement of the system excited with the scaled ground motion pair and averages of 11 ground motions pair are calculated.

4. RESULTS AND COMPARISON

The analyses results are presented as eight ADRS graphs which are shown in the following pages, in Figures. 4-7. ADRS graphs provide the base shear and displacement demands for the seismic isolation systems in the region under DD1 and DD2 design levels.

In general, base shear ratios change between 3.4 % -40% and maximum level is reached at DD1 level (Case 6). Furthermore, there is almost eight times difference in displacement (755 mm / 91 mm) among all cases. The shortest period (T=2 s) and the smallest yield ratio (5%) combination gives the maximum base shear ratio of the system. For the same yield level, system has the highest displacement capacity at the longest period. High deformation and high base shear values at above 4 s period (as in Case 5 and Case 6) are considered infeasible. ADRS graphs indicate that optimum isolation system period should be kept between 2.5-4 s considering the fact that the isolation system with a period of 2 s is not effective in terms of spectral acceleration reduction in the superstructure. Regarding the long period range, 5 s period may cause re-centering problems and may result in unfeasible displacement demands. Upper and lower bounds of displacement and base shear values are tabulated in Table 3.

Case 3 (Fig. 4) and Case 6 (Fig. 7) show the response of the system under two extreme ground motion levels and is worth comparing. Maximum base shear ratio is 40% and 12% under the excitation of the highest (Case 6) and the lowest levels (Case 3) of ground motion, respectively. Displacement range is between 217 mm and 755 mm with an average value of 190 mm between 2.5 and 4 s. for the Case 6. Displacement range is limited to 92 mm - 237 mm for Case 3. There is a similar proportional reduction in minimum base shear ratios, from 10% to 3.5%. There is almost 3.3 times difference between the maximum base shears of Case 3 and Case 6. The maximum displacement value of Case 3 is nearly equal to the minimum displacement of Case 6. The effect of yield levels which are above 10% is not significant on ADRS chart in Case 3 when the period is 3 s.

Case 5 and Case 6 portray the change in the response of the system when the soil type switches from ZC to ZD. At the stiff site, (Case 5) maximum and minimum base shear values are 25% less than those at softer soil site (Case 6). When period becomes longer at the stiff site, the effect of yield level increases and horizontal displacement lines are elongated. When

the soil is stiffer the effect of period and yield level both diminish. Displacement demand at soil site is 170 mm larger than it is at the stiff site. Similarly, difference in maximum displacement demand is not less than 100 mm at ADRS graphs under moderate hazard conditions (Case 3 and Case 4) as well. Consequently, at soft soil, seismic isolation systems with high fundamental period necessitate very high displacement capacity.

Table 2. Earthquake ground motion used in this study.

#	Event	Mw	Station	Rjb (km)	Soil Type
1	Düzce, Turkey 1999	7.14	LAMONT 362	23.41	ZC
2	Hector Mine 1999	7.13	ABY	41.81	ZC
3			JNT	50.42	ZC
4			29P	42.06	ZC
5	Chi-Chi, Taiwan-04	6.2	CHY024	19.67	ZC
6			CHY006	24.58	ZC
7			CHY029	25.75	ZC
8			CHY101	21.61	ZD
9			CHY030	30.46	ZD
10			CHY028	17.63	ZC
11	Darfield, New Zealand 2010	7	HVSCS	24.36	ZC
12			CSHS	43.6	ZC
13			OXZ	30.63	ZC
14			PPHS	18.73	ZD
15			CHHC	18.40	ZD
16			PRPC	24.55	ZD
17			HVS	24.36	ZC
18			CCCC	19.89	ZD
19			PRPC	24.55	ZD
20	Landers 1992	7.28	FVR	25.02	ZC
21			FHS	26.84	ZD
22	El Mayor-Cucapah, Mexico 2010	7.2	CISWSHN	31.79	ZC
23			E11	15.36	ZD
24			TAM	25.32	ZD
25			CHI	18.21	ZD
26			CXO	19.12	ZD
27	Imperial Valley-06 1979	6.53	DLT	22.03	ZD
28			E12	17.94	ZD
29	Superstition Hills-02 1987	6.54	ICC	18.20	ZD
30	Victoria, Mexico 1980	6.33	CHI	18.53	ZD

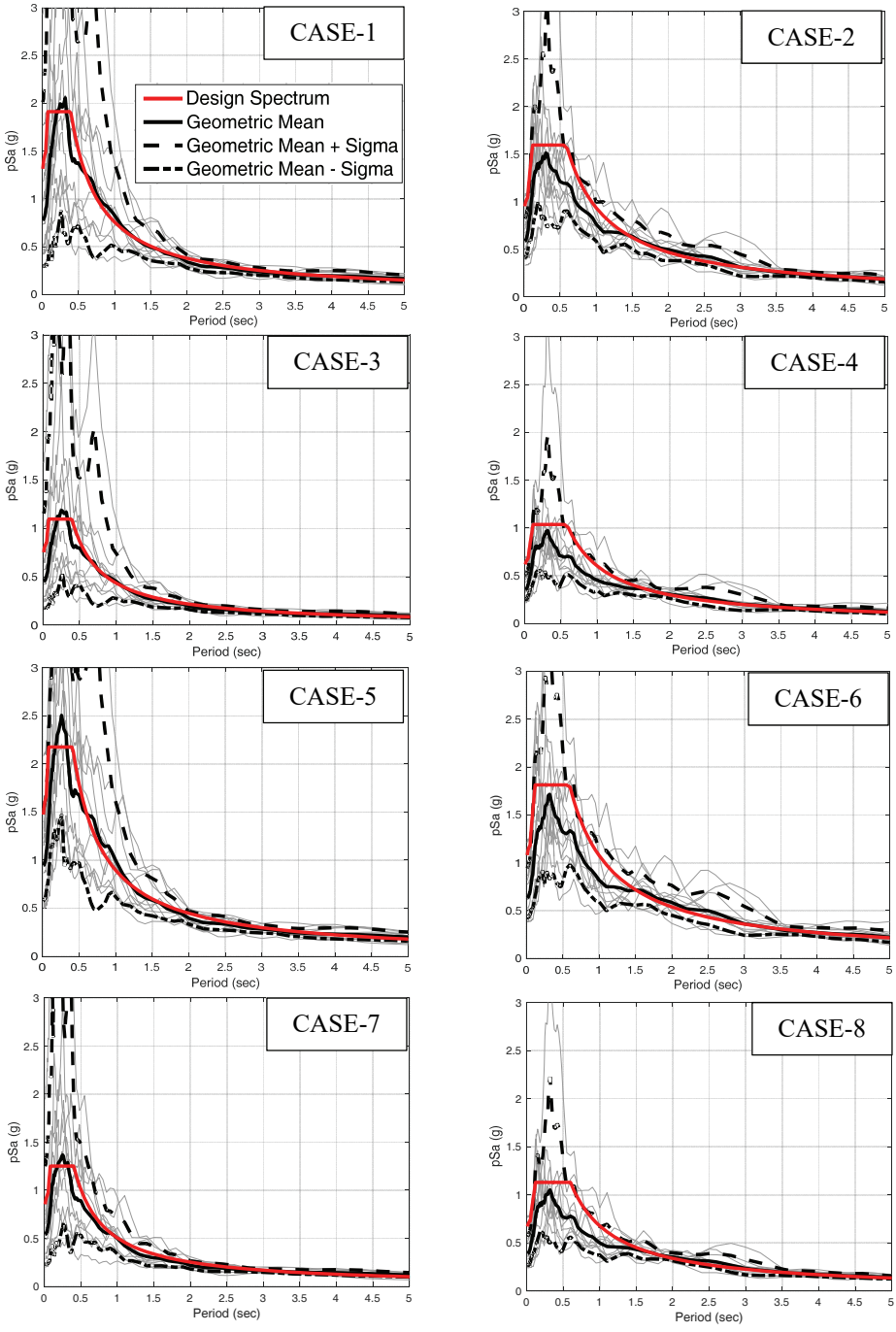

Figure 3 - Target design spectrum and spectra for scaled ground motions for Case 1-8

Fig. 7 shows the response of system for the Case 8. Base shear is around 20% and 5.7% for the smallest and largest period and yield ratio pairs, respectively. Displacements are between 105 mm and 409 mm. The effect of yield levels which are above 12.5% is not significant on ADRS chart when the period is 4 s. On the other hand, difference in yield level dominates the responses of the system at lower periods; 2.5 and 3 s.

Comparison of ADRS graphs for Case 6 and Case 8 reveals that, for the same soil condition, base shear imposed to superstructure under DD2 level is approximately half of that is imposed by DD1 level.

Table 3 - Upper and lower bounds of displacement and base shear

CASE #	**1**	**2**	**3**	**4**	**5**	**6**	**7**	**8**
Max. Displacement (mm)	494	647	237	341	595	**755**	274	409
Min. Displacement (mm)	166	176	92	95	226	217	91	105
Max. Base Shear (V/W)	0.25	0.33	0.12	0.18	0.31	**0.40**	0.14	0.21
Min. Base Shear (V/W)	0.07	0.09	0.03	0.05	0.08	0.11	0.04	0.06

Isolation system parameters of Sabiha Gökçen International Airport (SGIA) Terminal building and of two seismically isolated hospital buildings which are Okmeydanı Training and Research Hospital (OTRH) and Marmara University Başıbüyük Training and Research Hospital (BTRH) in Istanbul are compared with those calculated in this study. Triple-friction pendulum devices are used in SGIA Terminal building [24] and OTRH. Lead rubber bearings, sliding bearings and the pot bearing units are used in BTRH [17]. Implementation techniques of the isolators, main parameters which are taken into consideration and the other information for BTRH explained in related references [17, 25, 26].

Table 4 - Design parameters of seismically isolated structures in Istanbul, Turkey. Design parameters for hospitals (OTRH and BTRH) are provided from Bahadır Şadan (personal communication, 2018) and Sabiha Gökçen International Airport (SGIA) design parameters are provided from Zekioglu et al[19]

		OTRH	BTRH	SGIA
Distance to Fault (km)		>15	>15	>15
ADRS Chart		Case 2	Case 6	Case 5
Yield Strength Ratio (%)		10	15	13
Isolation Period (s.)		4	3	3
Displacement Demand (cm)	actual design	45	38	27-30
	this study	40	34	29

Comparison is tabulated in Table 4. For the given period and yield strength ratio the displacement values of ADRS graphs are consistent with the values used in the actual design, however a slight underestimation by ADRS graphs is observed. The boundary conditions which restrict structural design may sometimes lead to the extreme solutions of optimum area given in ADRS graphs. For instance, displacement demand needs to be increased due to the criterion of keeping the base shear force below a certain value. In this respect, it should be emphasized that the main argument in this research is not to precisely estimate the displacement demand but rather to determine the design solution envelope more quickly and effectively for preliminary phase.

5. CONCLUSION

In this paper, a parametric study is performed to determine the ideal parameters of seismic isolation systems at preliminary design phase. As generally accepted, bilinear force-displacement hysteresis curve is assumed to represent nonlinear behaviour of a typical seismic isolation system in a horizontal direction. A series of nonlinear time history analyses are performed for six post-elastic periods and five yield strength ratios of seismic isolation systems under the excitation of eleven ground motion pairs produced for eight cases. Each case is formed by the combination of design, hazard and site categories. Base shear is calculated through the average maximum displacement response. Finally, for the given yield strength ratio and isolation period, weight independent base shear versus displacement relationship is represented in ADRS graphs to provide optimal area for the preliminary design of the isolation systems. Graphs can be used for all typical seismic isolation systems since the calculations are solely based on post-elastic periods and yield levels.

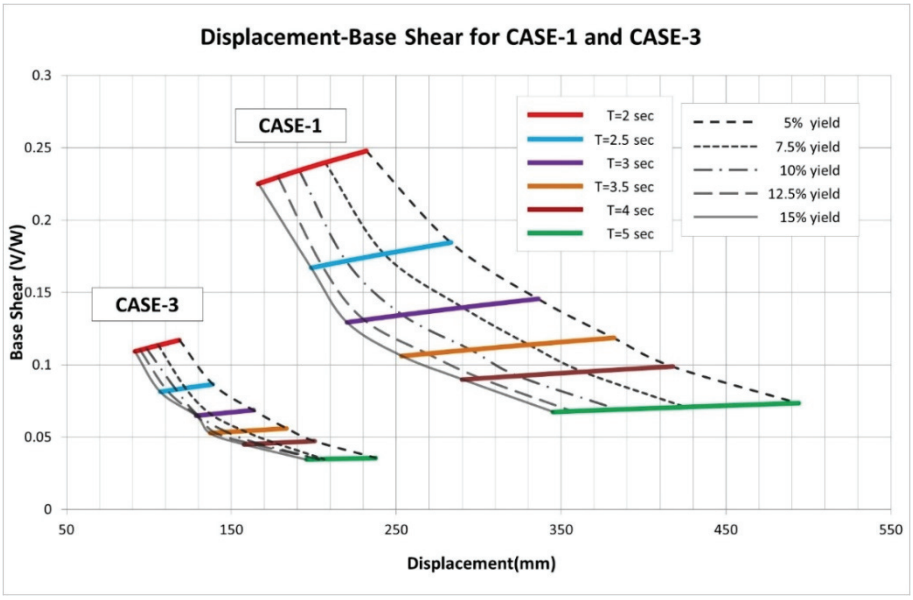

Figure 4 - Acceleration Displacement Response spectra for the Case1 and Case3

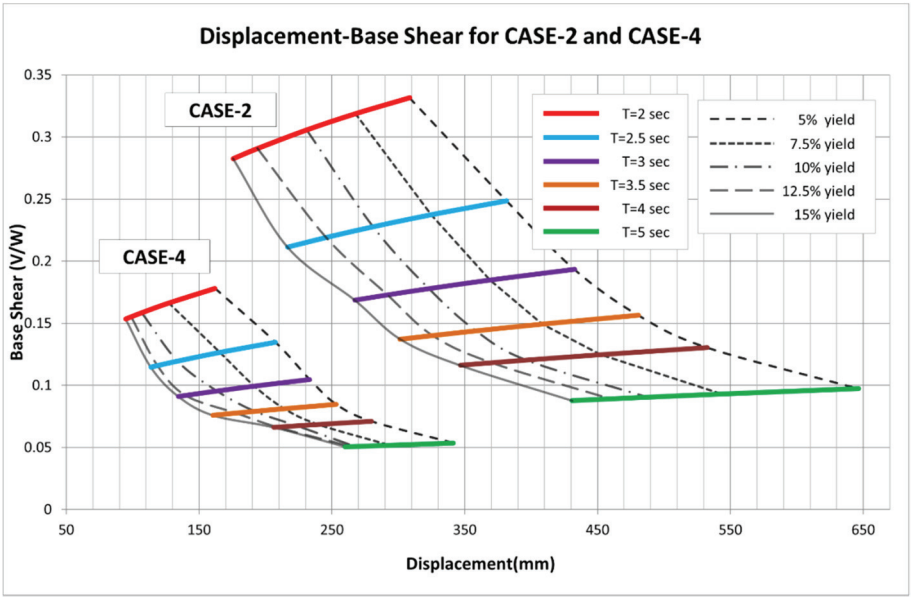

Figure 5 - Acceleration Displacement Response spectra for the Case2 and Case4

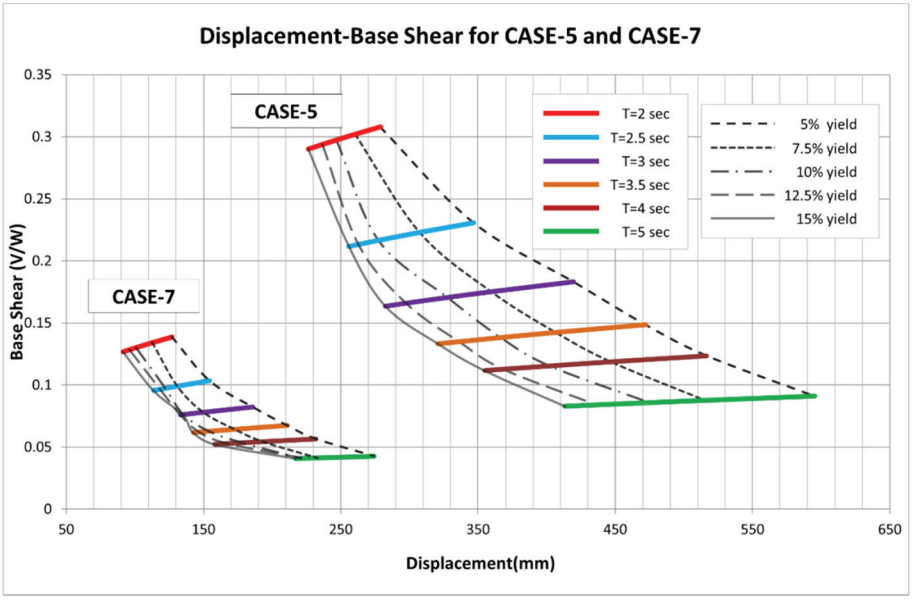

Figure 6 - Acceleration Displacement Response spectra for the Case5 and Case7

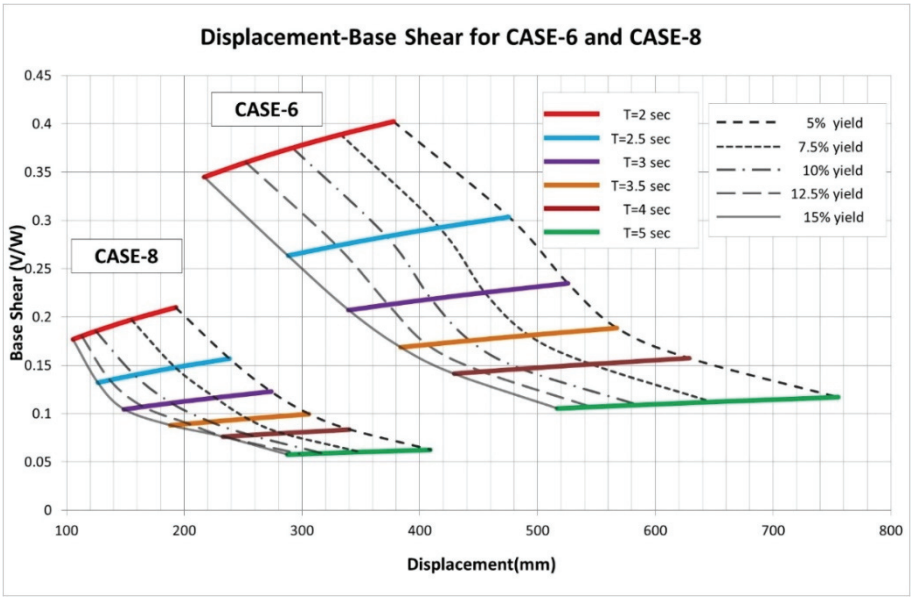

Figure 7 - Acceleration Displacement Response spectra for the Case6 and Case8.

It is worth noting that, only for Case 2; at T=3 s period, displacement responses are almost constant when yield levels are equal to or higher than 10%. In further studies, analyses might be repeated using different ground motion data set to see if such an issue is raised by the excitation characteristics of the ground motion.

Furthermore, it should also be kept in mind that, ADRS graphs presented in this study are valid under non-pulse far field ground motion excitation and may not be realistic at sites very close to active faults, particulary when the directionality effect is dominant in the ground motion recordings. Hence, this study can be expanded considering pulse-like ground motion sets.

Further studies can be focused on more detailed analysis with specific type of isolators such as high damping rubber bearing (HDRB), lead rubber bearing (LRB) and friction pendulum system (FPS) types.

Symbols

F_y Yield force

g Acceleration of gravity

k Stiffness

k_1 Elastic stiffness

k_2 Post-elastic stiffness

k_e	Effective stiffness
m_t	The total mass above the isolation device
M_w	Moment magnitude
Q_d	Strength on yield force
R	Earthquake force reduction factor
R_{jb}	Joyner and Boore distance
S_{ae}^{DD1}	Lateral spectral acceleration for 5% damping at maximum ground motion level (g)
S_{a1}	Hazard map spectral acceleration coefficient for 1 second period
T	Period
t	Time
T_M	The effective vibration period of seismically isolated building at maximum displacements
u	Displacement
u_{max}	Maximum deformation
u_y	Yield deformation
$u(t)$	Deformation of seismic isolation system
ü$_g(t)$	Ground acceleration
$\dot{u}$	Velocity of seismic isolation system
V_M	Base shear which is transmitted to superstructure
V_{s30}	The average shear wave velocity of top 30 meter depth.
W	System weight
z	Yielding history
η_M	Damping scaling coefficient
ξ	Damping ratio
ω	Circular frequency
ADRS	Acceleration-Displacement Response Spectra
DD1	Maximum Considered Earthquake
DD2	Design Basis Earthquake
HH	High hazard
MH	Moderate hazard
SDOF	Single degree of freedom
SRSS	Square root of the sum of the squares
TBSDC	Turkish Building Seismic Design Code
PEER	Pacific Earthquake Engineering Research

Acknowledgements

This study is supported by Boğaziçi University Research Fund Grant Number 13144. The subject matter is the MSc thesis of the first author. We thank to Mine B. Demircioğlu-Tümsa for preparing Fig.2.

References

[1] TASI, Turkish Association for Seismic Isolation. https://did.org.tr/, 2018.

[2] TBSDC-2018, Turkish Building Seismic Design Code, Disaster and Emergency Management Authority, Ankara, 2018.

[3] IBC 2015, International Building Code, International Code Council (ISBN: 978-1-60983-468-5), 2015.

[4] Anderson, E., and Mahin S. A., Displacement-based design of seismically isolated bridges, Proc. of the Sixth U.S. National Conference of Earthquake Engineering, Earthquake Engineering Research Institute, Oakland, California, 1998.

[5] Dicleli, M., Buddaram S., Comprehensive evaluation of equivalent linear analysis method for seismic-isolated structures represented by SDOF systems, Engineering Structures, Vol.29, 1653-1663, 2007.

[6] Park, J., and Otsuka, H., Optimal Yield Level of Bilinear Seismic Isolation Devices, Earthquake Engineering and Structural Dynamics, Vol. 28:941-955, 1999.

[7] Tena-Colugna A., A new method for the seismic design of structures with bilinear isolators using inelastic spectra, 12th World Conference on Earthquake Engineering, Auckland, New Zealand, 2000.

[8] Ryan, K. L., and Chopra A. K., Estimation of Seismic Demands on Isolators Based on Nonlinear Analysis, Journal of Structural Engineering,130 (3):392-402, ASCE, 2004.

[9] Whittaker, D., Jones, L., Design spectra for seismic isolation systems in Christchurch, New Zealand, NZSEE Conference, New Zealand, 2013.

[10] Whittaker, D., Jones, L., Displacement and acceleration design spectra for seismic isolation systems in Christchurch, New Zealand, NZSEE Conference, New Zealand, 2014.

[11] Jones, L., Aiken, I., Black, C., Whittaker, D., Design displacement and acceleration spectra for seismic isolation systems: New Zealand, San Francisco and Vancouver, 14th World Conference on Seismic Isolation, Energy Dissipation and Active Vibration Control of Structures, San Diego, CA USA, 2015.

[12] Jones, L., Aiken, I., Black, C., Whittaker, D., Ratemales, R., Boroschek, R., An improved design methodology for seismic isolation systems using nonlinear response spectra, 16th World Conference on Earthquake Engineering, Santiago, Chile, 2017.

[13] ASCE 7-10. Minimum design loads for buildings and other structures, American Society of Civil Engineers, Reston, 2010.

[14] Jones, L., Aiken, I., Black, C., Whittaker, D., Şadan, B., Nonlinear response spectra for isolation system design: case studies in Turkey, California and New Zealand, 3 TDMSK, Izmir, Turkey, 2015.

[15] NGA-West 2 Database (NGA-West2, 2015). Pacific Earthquake Engineering Research Center (PEER), University of California, Berkeley, USA(http://peer.berkeley.edu/ngawest2/).

[16] Naeim, F., and Kelly J. M., Design of Seismic Isolated Structures: From Theory to Practice, John Wiley & Sons, Chichester, UK, 1999.

[17] Erdik. M., Ülker, Ö., Şadan, B., Tüzün, C., Seismic isolation code developments and significant applications in Turkey, Soil Dynamics and Earthquake Engineering 115, 413-437, 2018.

[18] Eurocode 8, Design provisions for earthquake resistance of structures, ENV-2003, CEN, Brussels, 2003.

[19] Akkar, S., Azak T., Çan T., Çeken U., Demircioğlu Tümsa M. B., Duman, T. Y., Erdik, M., Ergintay, S., Kadirioğlu, F. T., Kalafat, D., Kale, Ö., Kartal R. F., Kekovalı K., Kılıç T. S., Zülfikar Ö., Evolution of seismic hazard maps in Turkey, Bulletin of Earthquake Engineering, Vol.16, Issue 8, pp 3567-3570, 2018.

[20] New Probabilistic Seismic Hazard Map of Turkey (TDTH, 2016) (https://tdth.afad.gov.tr/).

[21] Luco, N., and Bazzurro P. Does amplitude scaling of ground motion records result in biased nonlinear structural drift responses?, Earthquake Engineering and Structural Dynamics; 36 Issue13: 1813–35., 2007.

[22] Prism for Earthquake Engineering Software 2.0.1 (PRISM) 2018, Earthquake Engineering Research Group, Department of Architectural Engineering, INHA University, Incheon, South Korea, 2018.

[23] Erdik M., Seismic Isolation for Buildings, 6th National Conference on Earthquake Engineering, Istanbul, 16-20 October 2007.

[24] Zekioglu, A., Darama, H., Erkuş, B. Performance-based seismic design of a large seismically isolated structure: Istanbul Sabiha Gokcen International Airport Terminal Building., Proc. of the SEAOC 2009 Convention, San Diego, California, September 23-26, 2009.

[25] Sucuoğlu, H., Kubin, J., Kubin, D., Özmen, A., Şadan, B., Eroğlu, E., Seismic retrofit of an existing multi-block hospital by seismic isolators, 15WCEE Lisboa, Portugal, 2012.

[26] Sartori, M., Maraston, S., Zivanovic, I., Seismic retrofitting of the Marmara Başibüyük University Hospital in Istanbul, 16WCEE, Santiago Chile, 9-13 January 2017.